

External α carbonic anhydrase and solute carrier 4 (SLC4) bicarbonate transporter are required for HCO_3^- uptake in a freshwater angiosperm

Wenmin Huang¹, Shijuan Han¹, Hong Sheng Jiang¹, Shuping Gu², Li Wei¹, Brigitte Gontero³, and Stephen C. Maberly⁴

¹Chinese Academy of Sciences Key Laboratory of Aquatic Botany and Watershed Ecology

²Affiliation not available

³Aix-Marseille-University

⁴Centre for Ecology and Hydrology Lancaster

May 5, 2020

Abstract

Macrophyte productivity supports the littoral food web in fresh waters where widespread active CO_2 concentrating mechanisms (CCMs) allow their productivity to be maintained despite potential inorganic carbon limitation. We studied HCO_3^- acquisition, the most common CCM in macrophytes, in the freshwater monocot *Ottelia alismoides* and showed that the external carbonic anhydrase (CA) inhibitor acetazolamide (AZ) decreases the affinity for CO_2 uptake and prevents HCO_3^- use. The anion exchanger (AE)/solute carrier (SLC) type HCO_3^- transporters inhibitor 4,4'-diisothio-cyanatostilbene-2,2'-disulfonate (DIDS), has a smaller effect on CO_2 uptake but also prevents HCO_3^- use. Analysis of transcripts showed that putative $\alpha\text{CA-1}$ and SLC4 HCO_3^- transporters are unaffected by acclimation of leaves to different CO_2 , in agreement with physiological measurements showing a constitutive HCO_3^- use. Therefore, it is likely that $\alpha\text{CA-1}$ and SLC4 HCO_3^- transporters are the targets of AZ and DIDS, respectively. Altogether, these results are consistent with acquisition of HCO_3^- based on co-diffusion of CO_2 and HCO_3^- through the boundary layer, conversion of HCO_3^- to CO_2 at the plasmalemma by $\alpha\text{CA-1}$ and in addition, transport of HCO_3^- across the plasmalemma by SLC4 transporters. A model of these processes has been produced that can be used to test inorganic carbon uptake in future experiments.

KEYWORDS (5-10)

anion exchanger (AE), bicarbonate, carbonic anhydrase (CA), CO_2 concentrating mechanisms (CCMs), inorganic carbon acquisition, *Ottelia alismoides*, pH drift, photosynthesis, solute carrier 4 (SLC4)

1 | INTRODUCTION

Macrophytes form the base of the freshwater food web and are major contributors to primary production, especially in shallow systems (Silva et al., 2013; Maberly & Gontero, 2018). However, the supply of CO_2 for photosynthesis in water is potentially limited by the approximately 10,000 lower rate of diffusion compared to that in air (Raven, 1970). This imposes a large external transport resistance through the boundary layer (Black et al., 1981), that results in the K_d for CO_2 uptake by macrophytes to be 100-200 μM , roughly 6-11 times air-equilibrium concentrations (Maberly & Madsen, 1998). Furthermore, in productive systems the concentration of CO_2 can be depleted close to zero (Maberly & Gontero, 2017). Freshwater plants have evolved diverse strategies to minimize inorganic carbon (Ci) limitation (Klavnsen et al., 2011) including the active concentration of CO_2 at the active site of ribulose-1,5-bisphosphate carboxylase/oxygenase (Rubisco), collectively known as CO_2 concentrating mechanisms (CCMs). The most frequent CCM in freshwater plants

is based on the biophysical uptake of bicarbonate (HCO_3^-), which is present in ~50% of the species tested (Maberly & Gontero, 2017; Iversen et al., 2019). While CO_2 can diffuse through the cell membrane passively, HCO_3^- use requires active transport because the plasmalemma is impermeable to HCO_3^- and the negative internal membrane potential (Denny & Weeks, 1970) produces a large electrochemical gradient resisting passive HCO_3^- entry (Maberly & Gontero, 2018).

Detailed studies of the mechanisms of HCO_3^- use have been carried out in microalgae, marine macroalgae, seagrasses and to a lesser extent, freshwater macrophytes (Giordano et al., 2005). Direct uptake/transport of HCO_3^- can occur via an anion exchanger (AE) located at the plasmalemma (Sharkia et al., 1994). Inhibition of this protein by the membrane impermeable and highly specific chemical, 4,4'-diisothiocyanatostilbene-2,2'-disulfonate (DIDS), has confirmed its effect in a range of marine macroalgae and seagrasses (Drechsler et al., 1993; Björk et al., 1997; Fernández et al., 2014). Genomic studies have found probable AE proteins, from the solute carrier 4 (SLC4) family bicarbonate transporters (Romero et al., 2013), in marine microalgae (Nakajima et al., 2013; Poliner et al., 2015).

Carbonic anhydrase (CA) is a ubiquitous enzyme and is present in photosynthetic organisms. It interconverts CO_2 and HCO_3^- , maintaining equilibrium concentrations when rates of carbon transformation are high (Moroney et al., 2001; Dimario et al., 2018). External carbonic anhydrase (CA_{ext}) is inhibited by the impermeable inhibitor acetazolamide (AZ). The widespread nature of CA_{ext} is demonstrated by the inhibition of rates of photosynthesis in a range of aquatic photoautotrophs (James & Larkum, 1996; Larsson & Axelsson, 1999; Moroney et al., 2011; Tachibana et al., 2011; van Hille et al., 2014; Fernández et al., 2018). In many marine species, both CA_{ext} and an AE protein are implicated in the uptake of HCO_3^- but very little is known about freshwater macrophytes (Millhouse & Strother, 1986; Beer & Rehnberg, 1997; Björk et al., 1997; Gravot et al., 2010; Tsuji et al., 2017).

Ottelia alismoides (L.) Pers., a member of the monocot family Hydrocharitaceae, possesses two biochemical CCMs: constitutive C4 photosynthesis and facultative Crassulacean Acid Metabolism (CAM; Zhang et al., 2014; Shao et al., 2017; Huang et al., 2018). The leaves of *O. alismoides* comprise epidermal and mesophyll cells that contain chloroplasts and large air spaces but lack Kranz anatomy (Han et al., 2020). Although it is known that it can use HCO_3^- in addition to CO_2 , little is known about the mechanisms responsible for HCO_3^- uptake. We have addressed this issue, with Ci uptake measurements using the pH-drift technique, experiments with inhibitors of CA and AE and analysis of transcriptomic data.

2 | MATERIALS AND METHODS

2.1 Plant material and growth conditions

O. alismoides seeds were sown in soil from Donghu Lake, adjacent to the laboratory in Wuhan, and covered with sterile tap water with an alkalinity of about 2.2 mequiv L^{-1} as described (Huang et al., 2018). After a month, seedlings were placed in a 400-L tank (64 cm deep) receiving natural daylight in a glasshouse on the flat roof of the laboratory. The tap water in the tank was changed weekly and snails were removed daily. After nearly two months, the plants in the tank had produced many mature leaves. pH and temperature were measured every day with a combination pH electrode (E-201F, Shanghai Electronics Science Instrument Co., China) connected to a Thermo Orion Dual Star Benchtop pH/ISE Meter. The alkalinity was measured by Gran titration with a standard solution of HCl. CO_2 concentrations were calculated from pH, alkalinity, and temperature using the equations in Maberly (1996). Because of their high biomass the plants generated high pH values (8.3-9.7) and low concentrations of CO_2 (0.11-6.15 μM) in the tank. Information of the conditions in the tank is shown in Supplementary Data Table S1.

To examine whether HCO_3^- acquisition was affected by carbon limitation, in a separate experiment *O. alismoides* was incubated at high and low CO_2 concentration for 40 days in plastic containers within one of the tanks in the glasshouse as described previously (Zhang et al., 2014). The pH in the low CO_2 treatment (LC) ranged from 8.0 to over 9.8 and the CO_2 concentration ranged from 0.1 to 13 μM with a mean of 2.4 μM . For the high CO_2 treatment (HC), CO_2 -saturated tap water was added to the buckets twice each day in order to keep the pH between 6.7-6.8, producing CO_2 concentrations between 481-1110 μM with a mean

of 720 μM (Supplementary Data Table S1). These different CO_2 acclimated leaves were used to detect the effect of AZ and DIDS on Ci uptake rate and external CA activity.

2.2 pH-drift experiments

The pH-drift technique was used to determine the capacity of *O. alismoides* to utilize HCO_3^- , and the effects of inhibitors (AZ and DIDS) on photosynthetic Ci uptake (Maberly & Spence, 1983). Measurements were made in a glass and plastic chamber (Maberly, 1990) containing 121 mL of 1 mM HCO_3^- comprising equimolar concentration of NaHCO_3 and KHCO_3 , a pH electrode (model IP-600-9 Jenco Instruments, USA) and an oxygen electrode (Unisense OX-13298). The chamber was placed in a water bath maintained at 25 and illuminated from the side by fluorescent tubes that provided $75 \mu\text{mol photon m}^{-2} \text{ s}^{-1}$ (400-700 nm, Li-Cor sensor connected to a Li-Cor LI-1400 data logger). Prior to the start of the pH drift experiments, the leaves were collected from the tank in the glasshouse in the morning to avoid possible physiological differences caused by a light:dark rhythm of the plant, and then pieces of ~ 1.1 g fresh weight (FW) of leaf tissue were cut and rinsed in the medium placed in a constant temperature room at 25 ± 2 °C for around 1-4 hours before use. The medium in the incubation chamber was initially bubbled with N_2 to reduce O_2 concentration $\sim 100 \pm 20 \mu\text{M}$, which was detected by the oxygen electrode connected to an Unisense microsensor multimeter (Version 2.01) and recorded on a laptop computer. At the start of all drift experiments, the pH of the medium was set to 7.6 with CO_2 -bubbled medium, and the subsequent changes were measured with the pH electrode connected to a pH meter (model 6311, Jenco Instruments, USA), and recorded on a monitor (TP-LINK, TL-IPC42A-4). The pH-drifts, undertaken at least in triplicate, took 6-23 h to reach an end point value (final pH), which was deemed to be achieved when the pH changed less than 0.01 unit in one hour (Maberly, 1990). After each drift, the dry weight of the plant material and the alkalinity of the medium were measured, allowing Ci concentrations and Ci uptake rates to be calculated (Maberly & Spence, 1983). When photosynthetic Ci uptake rates were plotted against the total carbon concentration (C_T) at which the rate occurred, a two-phased response curve was observed. The linear response at higher C_T concentration was the consequence of CO_2 use, and the extrapolated intercept with the C_T axis corresponded to the CO_2 -compensation point (Maberly & Spence, 1983).

2.3 Effect of inhibitors on Ci-uptake and external CA activity

Inhibitors were used in pH-drift experiments to determine their effect on Ci-uptake. A stock solution of AZ (20 mM) was prepared by dissolving the solid in 20 mM NaOH and 0.61 or 1.21 mL was injected into the chamber to produce final concentration of 0.1 or 0.2 mM respectively. Stock solutions of 30 mM DIDS, were prepared daily by dissolving the powder in distilled water (Cabantchik & Greger, 1992), and 1.21 mL was injected into the chamber to produce a final concentration of 0.3 mM. Both stock solutions were kept in the dark at 4°C.

To check if the inhibitory effect of AZ on HCO_3^- uptake was reversible, we performed three consecutive drifts using the same *O. alismoides* leaf cut longitudinally into two halves. The first half was used as a control (first drift) without AZ. The second half was treated with AZ (second drift). Subsequently, this leaf and chamber were thoroughly rinsed with clean medium three times over ten minutes, and finally a post-control (third drift), was performed without the inhibitor. All the pH-drifts were started at pH 7.6 and stopped at pH 8.5 and replicated at least in triplicate.

2.4 External CA activity

The CA_{ext} activity was measured as in Fernández et al. (2018) with small modifications, using commercial CA (Sigma, C4396) as a positive control and to check activity linearity (Figure S1). A 50 mL plastic tube was placed inside a container filled with ice that maintained the temperature at 0-4°C. Approximately 60 mg FW leaf was placed in the tube containing 10 mL of buffer (pH 8.5): 50 mM Tris, 2 mM DTT, 15 mM ascorbic acid, 5 mM $\text{Na}_2\text{-EDTA}$ and 0.3% w/v polyvinylpyrrolidone (PVP). Temperature and pH were simultaneously measured using a pH meter. The reaction was started by rapidly introducing 5 mL of ice-cold CO_2 saturated water and pH was recorded over time. The relative enzyme activity (REA) was determined using the equation below:

$$\text{REA} = (T_b/T_s) - 1 \quad (1)$$

where T_b and T_s are the times in seconds required for the pH to drop from pH 8.3 to 7.9 in the non-catalyzed (without sample) and catalyzed reactions, respectively. The REA was expressed on a fresh weight basis. In the leaves grown at LC and HC, external CA activity was measured in the presence of 0.1 mM and 0.2 mM AZ as well as 0.3 mM DIDS.

2.5 Transcriptomic analysis

CA_{ext} and AE proteins were searched for within a transcriptome dataset obtained from *O. alismoides* acclimated to LC and HC (Huang et al., 2018). Information of the different CO₂ treatments is shown in Supplementary Data Table S1. Six samples (three HC and three LC acclimated mature leaves) were used for second-generation sequencing (SGS) for short but high-accuracy reads (Hackl et al., 2014). Six other samples were used for the third-generation sequencing (TGS) for longer sequences but lower-quality reads (Roberts et al., 2013).

Around 0.3 g fresh weight leaves were collected 30 minutes before the end of the photoperiod, flash frozen in liquid N₂ and stored at -80°C before use. Total RNA was extracted using a commercial kit RNAiso (Takara Biotechnology, Dalian, China). The purified RNA was dissolved in RNase-free water, with genomic DNA contamination removed using TURBO DNase I (Promega, Beijing, China). RNA quality was checked with the Agilent 2100 Bioanalyzer (Agilent Technologies, Palo Alto, California). Only the total RNA samples with RNA integrity numbers [?]8 were used to construct the cDNA libraries in PacBio or Illumina Hiseq sequencing.

For TGS analysis, total RNA (2 µg) was reversely transcribed into cDNA using the SMARTer PCR cDNA Synthesis Kit that has been optimized for preparing high-quality, full-length cDNAs (Takara Biotechnology, Dalian, China), followed by size fractionation using the BluePippin Size Selection System (Sage Science, Beverly, MA). Each SMRT bell library was constructed using 1-2 µg size-selected cDNA with the Pacific Biosciences DNA Template Prep Kit 2.0. SMRT sequencing was then performed on the Pacific Bioscience sequel platform using the manufacturer's protocol.

For SGS analysis, cDNA libraries were constructed using a NEBNext® Ultra RNA Library Prep Kit for Illumina(r) (NEB, Beverly, MA, USA), following the manufacturer's protocol. Qualified libraries were sequenced, and 150 bp paired-end reads were generated (Illumina Hiseq 2500, San Diego, CA, USA).

The TGS subreads were filtered using the standard protocols in the SMRT analysis software suite (<http://www.pacificbiosciences.com>) and reads of insert (ROIs) were generated. Full-length non-chimeric reads (FLNC) and non-full-length cDNA reads (NFL) were recognized through the identification of poly(A) signal and 5' and 3' adaptors. The FLNC reads were clustered and polished by the Quiver program with the assistance of NFL reads, producing high-quality isoforms (HQ) and low-quality isoforms (LQ). The raw Illumina reads were filtered to remove ambiguous reads with 'N' bases, adaptor sequences and low-quality reads. Filtered Illumina data were then used to polish the LQ reads using the proovread 213.841 software. The redundant isoforms were then removed to generate a high-quality transcript dataset for *O. alismoides*, using the program CD-HIT.

TransDecoder v2.0.1 (<https://transdecoder.github.io/>) was used to define the putative coding sequence (CDS) of these transcripts. The predicted CDS were then functional annotated and confirmed by BLAST, which was conducted against the following databases: NR, NT, KOG, COG, KEGG, Swissprot and GO. For each transcript in each database searched, the functional information of the best matched sequence was assigned to the query transcript. The phylogenetic tree of αCA-1 isoforms based on deduced CA peptide sequences from the NCBI, was analyzed with Geneious software (Windows version 11.0, Biomatters Ltd, New Zealand). The location of the protein was analyzed using Target P1 (Emanuelsson et al., 2007; <http://www.cbs.dtu.dk/services/TargetP/>).

2.6 Statistical analysis

All data presented in this study are the mean \pm SD. Mean final pH values were calculated geometrically. One-way ANOVA was used to test for significant variation, after homogeneity and normality were satisfied. Duncan's and Tukey's post-hoc tests were used to test for significance among treatments while percentage data were compared using a non-parametric Mann-Whitney test. The threshold of statistical significance was set at $P < 0.05$. The data were analyzed using SPSS 16.0 (SPSS Inc., Chicago, IL, USA).

3 | RESULTS

In control leaves, the pH drift end point was reached after nearly 24 hours at a mean pH of 10.2 (Figure 1, Figure 2a) and a very low final CO_2 concentration of $\sim 0.03 \mu\text{M}$ (about 450-fold below air equilibrium, and at an oxygen concentration of about $353 \mu\text{M}$, about 137% of air-equilibrium; Figure 2b) indicating that HCO_3^- had been used. In leaves treated with AZ or DIDS, the pH drift stopped after 6 to 12 hours and the end point did not exceed pH 9.3; final CO_2 concentrations were between 0.8 and $1.6 \mu\text{M}$ (Figure 1, Figure 2a,b), indicating that HCO_3^- use had been inhibited. As a consequence of HCO_3^- use in control leaves, rates of Ci uptake were about $40 \mu\text{mol g}^{-1} \text{DW h}^{-1}$ even at the very low CO_2 concentrations (Figure S2). The slope of Ci uptake *vs* concentration of CO_2 between 15 and $40 \mu\text{M}$ in leaves treated with AZ was between 54.1% and 70.6% lower than the control ($P < 0.05$) and in leaves treated with DIDS, it was about 35% lower than the control ($P < 0.05$; Figure 2c). In contrast, the intercept CO_2 compensation points increased significantly as a result of the addition of AZ (Figure 2d). The higher AZ concentration treatments had a CO_2 compensation concentration close to $20 \mu\text{M}$ (at an oxygen concentration of $163 \mu\text{M}$) suggesting that CCM is absent. These results suggest that AZ not only inhibited CA_{ext} but also inhibited the AE protein. The CO_2 compensation concentration in the presence of DIDS, at about $5 \mu\text{M}$ (at an oxygen concentration of $232 \mu\text{M}$, about 90% of air-equilibrium), was not significantly different from the control but substantially lower than in the two AZ treatments (Figure 2d). The $\text{C}_T/\text{alkalinity}$ quotient (the remaining total Ci at the end of the drift, C_T related to the alkalinity) is a measure of the effectiveness of Ci depletion. A low quotient indicates that a large proportion of the Ci pool is available for acquisition and vice versa. While HCO_3^- use in control leaves allowed about half of the available inorganic carbon to be accessible, in the AZ and DIDS treated leaves, a high quotient was obtained and only between 11 and 16% of the available inorganic carbon was accessible (Figure 2e).

Figure 3 shows the Ci uptake rates at different CO_2 concentrations calculated from the pH-drift experiments over a pH range from about 7.7 to 9.3. AZ inhibited Ci-uptake at all the CO_2 concentrations (Figure 3a), and both AZ concentrations inhibited Ci uptake by between 70 and 76% when the concentrations of CO_2 were between 2.6 and $11 \mu\text{M}$. In contrast, DIDS did not affect Ci uptake at CO_2 concentrations above $4.2 \mu\text{M}$ but inhibited Ci uptake by about 40% at CO_2 concentrations between about 1 and $4 \mu\text{M}$ (Figure 3b). The inhibitory effect caused by AZ at both concentrations, can be completely reversed by washing since the post-control rates of Ci uptake were not significantly different from the initial control ($P > 0.05$; Figure 4). This confirms that AZ does not penetrate the plasmalemma (Moroney et al., 1985) and thus that the observed effects are linked to inhibition of CA_{ext} .

The inhibition of Ci uptake rates in the presence of 0.1 mM AZ and 0.3 mM DIDS were not significantly different in leaves acclimated to HC *vs* LC, although there was a slightly greater inhibition by 0.2 mM AZ in HC compared to LC leaves ($P < 0.05$; Figure 5a,b). CA_{ext} activity was present in both HC and LC leaves but it was greater in LC leaves ($P < 0.01$; Figure 5c). CA_{ext} activity was inhibited by AZ: the 0.2 mM treatment caused a greater inhibition than 0.1 mM AZ (Figure 5d). DIDS had no effect on CA_{ext} activity neither in HC nor in LC leaves. Ci uptake rates, measured at an initial CO_2 concentration of $12 \mu\text{M}$, were broadly positively related to the activity of CA_{ext} ($R^2 = 0.84$ and 0.74 for HC and LC leaves respectively, $P < 0.01$).

The inhibition of Ci uptake in *O. alismoides* by AZ and DIDS implied that both CA_{ext} and anion exchange protein were present. This was characterized further using transcriptomic analysis: mRNA for putative alpha carbonic anhydrase 1 ($\alpha\text{CA-1}$) and HCO_3^- transporters were expressed. Fifty-three transcripts were functionally annotated to CA according to sequence similarity and translated into 66 peptides. Six of these peptides were homologous with αCA1 based on a comparison of amino acid sequences with the NCBI database and corresponded to four CA isoforms (Figure 6a, Figure S3). Isoform 1 in *O. alismoides* shows

60% and 61% identity with the chloroplastic isoform X1 and X2 of α CA-1 from the monocot *Musa acuminata*. Isoforms 2, 3 and 4 show 58%, 55% and 56% identity with the isoform X1 from this species, respectively, as well as 59%, 57% and 58% identity with the isoform X2. However, according to Target P1 software, all the isoforms from *O. alismoides* were predicted to be localized in the secretory pathway (Figure 6b). The expression of the four isoforms of putative α CA-1, was not significantly different in HC and LC acclimated leaves ($P > 0.05$, Figure 6c).

Unfortunately, transcripts of HCO_3^- transporters were not detected due to the lower sensitivity of TGS, but were present in the dataset from SGS. Fifteen peptides sequences (Figure S3) were inferred to be homologous to HCO_3^- transporter family with the following dicot species in the database: *Artemisia annua* (70.6-78.9%), *Corchorus olitorius* (73.1-85.7%), *Corchorus capsularis* (73.1-85.7%), *Cynara cardunculus* (80.4-85.7%), *Lupinus albus* (73.22%), *Macleaya cordata* (76.2-83.5%), *Parasponia andersonii* (74.0%), *Populus alba* (77.6%), *Prunus dulcis* (78.5-82.4%), *Striga asiatica* (81.6-83.5%), *Theobroma cacao* (79.2-85.0%) and *Trema orientale* (75.1-75.8%). This HCO_3^- transporter family contains Band 3 anion exchange proteins, which also known as anion exchanger 1 or SLC4 member 1. Only partial sequences could be deduced from our analysis and since the peptides for putative HCO_3^- transporters are membrane proteins, their location could not be predicted. The mRNA expressions of all the transcripts for putative SLC4 HCO_3^- transporters were not significantly different in HC and LC acclimated leaves ($P > 0.05$, data not shown); the expression-data for the highest expressed transcript for SLC4 HCO_3^- transporters is presented in Figure 6d.

4 | DISCUSSION

O. alismoides possesses three CCMs, including constitutive abilities to (i) use HCO_3^- and (ii) operate C4 photosynthesis, and a facultative ability to perform CAM when acclimated to low CO_2 concentrations (Zhang et al., 2014; Shao et al., 2017; Huang et al., 2018). We confirm here that this species has a constitutive ability to use HCO_3^- , and this allows it to exploit a large proportion of the C_i pool and drive CO_2 to very low concentrations.

In this study, multiple lines of evidence show that an external CA, putative α CA-1, plays a major role in C_i uptake in *O. alismoides*: (i) external CA activity was measured, (ii) AZ inhibited C_i uptake with the slope of C_i uptake vs the concentration of CO_2 between 15 and 40 μM being about a quarter of the control after treatment with 0.2 mM AZ, (iii) transcripts of putative α CA-1 were detected. The CA was confirmed to be external since (i) washing of leaves treated with AZ, restored CA activity and (ii) its sequence bears a signal peptide consistent with a periplasmic location. External CA is indeed widespread in photoautotrophs from marine and freshwater environments (Moroney et al., 2001; Dimario et al., 2018). The green microalga *Chlamydomonas reinhardtii* has three α CAs, of which two (Cah1 and Cah2) are localized in the periplasmic space and one (Cah3) in the thylakoid membrane (Fujiwara et al., 1990; Karlsson et al., 1998; Moroney & Chen, 1998). While CAs have the same catalytic activity, their sequence identity could be very low among different classes (Jensen et al., 2019). The α CA-1 from *O. alismoides* has around 30% sequence identity with the periplasmic Cah1 from *C. reinhardtii*. Many CAs are regulated by the concentration of CO_2 . The diatom *Phaeodactylum tricornutum* does not possess external CA, but the internal CA (β -type CA) is CO_2 responsive and crucial for its CCM operation (Satoh et al., 2001; Harada et al., 2005; Harada & Matsuda, 2005; Tsuji et al., 2017). In the marine diatom, *Thalassiosira pseudonana*, the two external CAs, δ -CA and ζ -CA, as well as a recently identified chloroplastic ι -CA are induced by carbon limitation (Samukawa et al., 2014; Clement et al., 2017; Jensen et al., 2019). In contrast, the putative α CA-1 in *O. alismoides* is constitutive and its expression was unaffected by the CO_2 concentration. This is also true for Cah3 in the thylakoid lumen of *C. reinhardtii* (Karlsson et al., 1998; Moroney & Chen, 1998), while the expression of the periplasmic CA (Cah1) and the mitochondrial CAs (β -CA1 and β -CA2) are highly CO_2 -sensitive (Moroney & Chen, 1998).

We show that the anion exchange proteins, one group of the SLC4 family HCO_3^- transporters (Romero et al., 2013), is involved in HCO_3^- uptake in *O. alismoides*. DIDS, a commonly-used inhibitor of AE/SLC-type HCO_3^- transporters (Romero et al., 2013) significantly decreased the final pH of a drift, and increased the final CO_2 concentration to about 0.8 μM which is not substantially less than that expected in the

absence of a CCM: a terrestrial C₃ plant CO₂ compensation point of 36 $\mu\text{L L}^{-1}$ (Bauer & Martha, 1981) is equivalent to about 1.2 μM . Furthermore, transcripts of putative HCO₃⁻ transporter family in *O. alismoides* were found to contain Band 3 anion exchange proteins (SLC4 member 1), and the peptides shared 70.6-85.7% sequence identity with HCO₃⁻ transporters from other terrestrial plant species. Several genes which encode SLC4 family transporters, has been found to be involved in the CCMs in the marine microalgae *Phaeodactylum tricornutum* and *Nannochloropsis oceanica* (Nakajima et al., 2013; Poliner et al., 2015), as well as the marine macroalga *Ectocarpus siliculosus* (Gravot et al., 2010). More broad evidence from the physiological data have demonstrated that anion exchange proteins play a role in HCO₃⁻ uptake in green, red and brown marine macroalgae (Drechsler et al., 1993; Granbom & Pedersén, 1999; Larsson & Axelsson, 1999; Fernández et al., 2014). Although HCO₃⁻ use by seagrasses is known to involve an anion exchange protein, to our knowledge, this is the first report that provides evidence of the presence of a direct HCO₃⁻ uptake via DIDS-sensitive SLC4 HCO₃⁻ transporters in an aquatic angiosperm. Whatever, these transporters for direct HCO₃⁻ acquisition, appears to be much more restricted in distribution than the widespread external CA.

Three mechanisms of HCO₃⁻ use have been proposed in aquatic plants: i) indirect use of HCO₃⁻ based on dehydration of HCO₃⁻, facilitated by external CA, to produce elevated CO₂ concentrations outside the plasmalemma; ii) direct uptake of HCO₃⁻ by an anion exchange transporter in the plasmalemma and iii) direct uptake of HCO₃⁻ by a P-type H⁺-ATPase (Giordano et al., 2005). In this study we provide evidence for the first two mechanisms in *O. alismoides*. Although we did not specifically check for a P-type H⁺-ATPase, this process appears to be absent, or of minor importance, in *O. alismoides* in contrast to *Laminaria digitata* and *L. saccharina* (Klenell et al., 2004), because in *O. alismoides*, HCO₃⁻ use was abolished by addition of either AZ or DIDS. An AE is mainly responsible for HCO₃⁻ use in the brown marine macroalga *Macrocystis pyrifera* (Fernández et al., 2014), while in several other brown macroalgae such as *Saccharina latissima* (formerly *Laminaria saccharina*) external CA plays the major role in HCO₃⁻ use (Axelsson et al., 2000), though in *L. saccharina* as in *L. digitata*, a P-type H⁺-ATPase has been identified (Klenell et al., 2004). In another brown macroalga, *Endarachne binghamiae*, HCO₃⁻ use was based on an external CA and P-type H⁺-ATPase with no contribution from an AE (Zhou & Gao, 2010). Another strategy to use HCO₃⁻ has been shown in some species of freshwater macrophytes that involves the possession of ‘polar leaves’ (Steemann-Nielsen, 1947). At the lower surface of these leaves, proton extrusion generates low pH and at their upper surface, high pH often generates calcite precipitation (Prins et al., 1980). Consequently, at the lower surface with low pH, the conversion of HCO₃⁻ to CO₂ near the plasmalemma facilitates the cells to take up Ci. Because of this, there is some evidence for a lower reliance on external CA in macrophytes with polar leaves. For example, in a species with polar leaves, *Potamogeton lucens*, external CA was absent (Staal et al., 1989) and in the polar leaf species *Elodea canadensis*, external CA activity was present but not influenced by the CO₂ concentration (Elzenga & Prins, 1988).

It was initially surprising that AZ completely inhibited HCO₃⁻ use. However, Sterling et al. (2001) also found that AZ inhibited AE1-mediated chloride-bicarbonate exchange. This result could be explained by the binding of CA to the AE resulting in the formation of a transport metabolon, where there was a direct transfer of HCO₃⁻ from CA active site to the HCO₃⁻ transporter (Sowah & Casey, 2011; Thornell & Bevenssee, 2015). Thus, when CA is inhibited, then the transport of HCO₃⁻ is inhibited.

O. alismoides can perform C4 photosynthesis, however the final CO₂ concentration at the end of pH-drift, when HCO₃⁻ use was abolished by the inhibitors, was 0.8-1.6 μM , which could be supported by passive entry of CO₂ without the need to invoke a CCM. These are slightly higher than the CO₂ compensation point in the freshwater C4 macrophyte *Hydrilla verticillata* at less than 10 ppm (Bowes, 2010), which is equivalent to a dissolved CO₂ 0.3 μM at 25 °C. If this difference between the species is real and not methodological, it could suggest that in *O. alismoides* C4 photosynthesis is more important to suppress photorespiration than to uptake carbon.

A simple model of carbon acquisition (Figure 7a) was constructed to quantify the contribution of the three pathways involved in Ci uptake in *O. alismoides*: passive diffusion of CO₂, HCO₃⁻ use involving $\alpha\text{CA-1}$ and HCO₃⁻ use involving SLC4 HCO₃⁻ transporters. Using the Ci uptake rates at different CO₂ concentrations

in Figure 3, and assuming that 0.3 mM DIDS completely inhibited HCO_3^- transporters and that 0.2 mM AZ completely inhibited $\alpha\text{CA-1}$ and HCO_3^- -transporters, we calculated: i) passive diffusion of CO_2 as the rate in the 0.2 mM AZ treatment that inhibited both $\alpha\text{CA-1}$ and SLC4 HCO_3^- transporters; ii) diffusion of HCO_3^- and conversion to CO_2 by $\alpha\text{CA-1}$ at the plasmalemma as the difference between the rate in the presence of 0.3 mM DIDS and that in the presence of 0.2 mM AZ; and iii) diffusion of HCO_3^- and transfer across the plasmalemma by SLC4 HCO_3^- transporters as the difference in the rate between the control and the 0.3 mM DIDS treatment. At a CO_2 concentration of about 50 μM , passive diffusion of CO_2 contributed 55.7% to total Ci uptake, diffusion of HCO_3^- and conversion to CO_2 by $\alpha\text{CA-1}$ contributed 42.7% and transfer of HCO_3^- across the plasmalemma by SLC4 HCO_3^- transporters contributed 1.6% (Figure 7b). At $\sim 9 \mu\text{M}$ (about 66% of equilibrium with air at 400 ppm CO_2) the contribution to total Ci uptake of CO_2 -diffusion, HCO_3^- diffusion and conversion to CO_2 by $\alpha\text{CA-1}$ and transfer by SLC4 HCO_3^- transporters was 24.0%, 64.4% and 11.5% respectively and at about 1 μM CO_2 (close to a typical C3 CO_2 compensation point) diffusion was zero and $\alpha\text{CA-1}$ and SLC4 HCO_3^- transporters contributed equally to carbon uptake. So, as CO_2 concentrations fall, passive CO_2 diffusion can no longer support Ci uptake and indirect and direct use of HCO_3^- allows Ci uptake to continue. The stimulation of absolute rates of SLC4 HCO_3^- transporters-dependent Ci uptake is consistent with patterns seen for a number of freshwater macrophytes during pH-drift experiments, where rates increase as CO_2 approaches zero before declining as Ci is strongly depleted (Maberly & Spence, 1983). This could be caused by regulation or by direct effects of pH on HCO_3^- transporters activity.

These results confirm the prevailing notion from seagrasses that external CA plays an important role in contributing to Ci uptake. External CA contributed 25% to Ci uptake in *Posidonia australis* (James & Larkum, 1996) and $\sim 60\%$ in *Zostera marina* (approximately 2.2 mM Ci at pH 8.2, equivalent to a dissolved $\text{CO}_2 \sim 23 \mu\text{M}$ at 25 °C; Beer & Rehnberg, 1997), albeit in the presence of Tricine buffer that might inhibit the photosynthesis rate. The value reported here for *O. alismoides* at a CO_2 concentration of 23 μM , 56%, is similar to *Z. marina*.

In conclusion, *O. alismoides* has developed a jack of trades CCM, the master of which, either external CA or SLC4 HCO_3^- transporters, depends on the CO_2 concentration. There are several future lines of work that need to be pursued. The distribution of HCO_3^- -transporters in freshwater species should be determined. The apparent relationship between polar leaves and low or absent external CA activity could be tested using a range of species, especially within the genus *Ottelia* where calcite precipitation differs among species (Cao et al., 2019). The Ci acquisition mechanisms of more freshwater species should be examined. The cause of the increasing rate of HCO_3^- transporters-dependent HCO_3^- uptake as Ci becomes depleted needs to be understood. Finally, production and analysis of genome sequences for freshwater macrophytes will be a powerful tool to answer these and future questions concerning the strategies used by freshwater macrophytes to optimize photosynthesis.

ACKNOWLEDGEMENTS

This work was supported by the Strategic Priority Research Program of the Chinese Academy of Sciences (Grant No. XDB31000000), Chinese Academy of Sciences President's International Fellowship Initiative to SCM and BG (2015VBA023, 2016VBA006), and the National Natural Science Foundation of China (Grant No. 31970368).

REFERENCES

- Axelsson, L., Mercado, J. M., & Figueroa, F. L. (2000). Utilization of HCO_3^- at high pH by the brown macroalga *Laminaria saccharina*. *European Journal of Phycology*, 35, 53–59. <https://doi.org/10.1080/09670260010001735621>
- Bauer, H., & Martha, P. (1981). The CO_2 compensation point of C3 plants - A re-examination I. Interspecific variability. *Zeitschrift für Pflanzenphysiologie*, 103, 445–450. [https://doi.org/10.1016/S0044-328X\(81\)80167-5](https://doi.org/10.1016/S0044-328X(81)80167-5)
- Beer, S., & Rehnberg, J. (1997). The acquisition of inorganic carbon by the seagrass *Zostera marina*. *Aquatic*

Botany , 56, 277–283. [https://doi.org/ 10.1016/S0304-3770\(96\)01109-6](https://doi.org/10.1016/S0304-3770(96)01109-6)

Björk, M., Weil, A., Semesi, S., & Beer, S. (1997). Photosynthetic utilization of inorganic carbon by seagrasses from Zanzibar, East Africa. *Marine Biology* , 129, 363–366. [https://doi.org/ 10.1007/s002270050176](https://doi.org/10.1007/s002270050176)

Black, M. A., Maberly, S. C., & Spence, D. H. N. (1981). Resistance to carbon dioxide fixation in four submerged freshwater macrophytes. *New Phytologist* , 89, 557–568. [https://doi.org/ 10.1111/j.1469-8137.1981.tb02335.x](https://doi.org/10.1111/j.1469-8137.1981.tb02335.x)

Bowes, G. (2010). Chapter 5 Single-Cell C₄ Photosynthesis in Aquatic Plants. In: Raghavendra, A., & Sage, R. (eds) C₄ Photosynthesis and Related CO₂ Concentrating Mechanisms. *Advances in Photosynthesis and Respiration*, 32, 63–80. Springer, Dordrecht. [https://doi.org/ 10.1007/978-90-481-9407-0_5](https://doi.org/10.1007/978-90-481-9407-0_5)

Cabantchik, Z. I., & Greger, R. (1992). Chemical probes for anion transporters of mammalian cell membranes. *American Journal of Physiology*, 262, C803–C827. [https://doi.org/ 10.1152/ajpcell.1992.262.4.C803](https://doi.org/10.1152/ajpcell.1992.262.4.C803)

Cao, Y., Liu, Y., Ndirangu, L., Li, W., Xian, L., & Jiang, H. S. (2019). The analysis of leaf traits of eight *Ottelia* populations and their potential ecosystem functions in Karst freshwaters in China. *Frontiers in Plant Science* , 9, 1938. [https://doi.org/ 10.3389/fpls.2018.01938](https://doi.org/10.3389/fpls.2018.01938)

Clement, R., Lignon, S., Mansuelle, P., Jensen, E., Pophillat, M., Lebrun, R., Denis, Y., Puppo, C., Maberly, S. C., & Gontero, B. (2017). Responses of the marine diatom *Thalassiosira pseudonana* to changes in CO₂ concentration: a proteomic approach. *Scientific Reports* , 7, 42333. <https://doi.org/10.1038/srep42333>

Denny, P., & Weeks, D. C. (1970). Effects of light and bicarbonate on membrane potential in *Potamogeton schweinfurthii* (Benn). *Annals of Botany* , 34, 483–496. [https://doi.org/ 10.1093/oxfordjournals.aob.a084384](https://doi.org/10.1093/oxfordjournals.aob.a084384)

DiMario, R. J., Machingura, M. C., Waldrop, G. L., & Moroney, J. V. (2018). The many types of carbonic anhydrases in photosynthetic organisms. *Plant Science* , 268, 11–17. [https://doi.org/ 10.1016/j.plantsci.2017.12.002](https://doi.org/10.1016/j.plantsci.2017.12.002)

Drechsler, Z., Sharkia, R., Cabantchik, Z. I., & Beer, S. (1993). Bicarbonate uptake in the marine macroalga *Ulva* sp. is inhibited by classical probes of anion exchange by red blood cells. *Planta* , 191, 34–40. <https://doi.org/10.1007/BF00240893>

Elzenga, J. T. M., & Prins, H. B. A. (1988). Adaptation of *Elodea* and *Potamogeton* to different inorganic carbon levels and the mechanism for photosynthetic bicarbonate utilization. *Australian Journal of Plant Physiology* , 15, 727–735. [https://doi.org/ 10.1071/PP9880727](https://doi.org/10.1071/PP9880727)

Emanuelsson, O., Brunak, S., von Heijne, G., & Nielsen, H. (2007). Locating proteins in the cell using TargetP, SignalP and related tools. *Nature Protocol* , 2, 953–971. [https://doi.org/ 10.1038/nprot.2007.131](https://doi.org/10.1038/nprot.2007.131)

Fernández, P. A., Hurd, C. L., & Roleda, M. Y. (2014). Bicarbonate uptake via an anion exchange protein is the main mechanism of inorganic carbon acquisition by the giant kelp *Macrocystis pyrifera* (Laminariales, Phaeophyceae) under variable pH. *Journal of Phycology* , 50, 998–1008. [https://doi.org/ 10.1111/jpy.12247](https://doi.org/10.1111/jpy.12247)

Fernández, P. A., Roleda, M. Y., Rautenberger, R., & Hurd, C. L. (2018). Carbonic anhydrase activity in seaweeds: overview and recommendations for measuring activity with an electrometric method, using *Macrocystis pyrifera* as a model species. *Marine Biology* , 165, 88. <https://doi.org/10.1007/s00227-018-3348-5>

Fujiwara, S., Fukuzawa, H., Tachiki, A., & Miyachi, S. (1990). Structure and differential expression of 2 genes encoding carbonic-anhydrase in *Chlamydomonas reinhardtii*. *Proceedings of the National Academy of Sciences USA* , 87, 9779–9783. [https://doi.org/ 10.1073/pnas.87.24.9779](https://doi.org/10.1073/pnas.87.24.9779)

Giordano, M., Beardall, J., & Raven, J. A. (2005). CO₂ concentrating mechanisms in algae: mechanisms, environmental modulation, and evolution. *Annual Review of Plant Biology* , 56, 99–131. [https://doi.org/ 10.1146/annurev.arplant.56.032604.144052](https://doi.org/10.1146/annurev.arplant.56.032604.144052)

Granbom, M., & Pedersén, M. (1999). Carbon acquisition strategies of the red alga *Eucheuma denticulatum*. *Hydrobiologia*, 398/399, 349–354. <https://doi.org/10.1023/A:1017059607075>

Gravot, A., Dittami, S. M., Rousvoal, S., Lugan, R., Eggert, A., Collen, J., Boyen, C., Bouchereau, A., & Tonon, T. (2010). Diurnal oscillations of metabolite abundances and gene analysis provide new insights into central metabolic processes of the brown alga *Ectocarpus siliculosus*. *New Phytologist*, 188, 98–110. <https://doi.org/10.1111/j.1469-8137.2010.03400.x>

Hackl, T., Hedrich, R., Schultz, J., & Förster, F. (2014). Proovread: large-scale high-accuracy pacbio correction through iterative short read consensus. *Bioinformatics*, 30, 3004–3011. <https://doi.org/10.1093/bioinformatics/btu392>

Han, S. J., Maberly, S. C., Gontero, B., Xing, Z. F., Li, W., Jiang, H. S., & Huang, W. M. (2020). Structural basis for C4 photosynthesis without Kranz anatomy in leaves of the submerged freshwater plant *Ottelia alismoides*. *Annals of Botany*. doi: <https://doi.org/10.1093/aob/mcaa005>

Harada, H., & Matsuda, Y. (2005). Identification and characterization of a new carbonic anhydrase in the marine diatom *Phaeodactylum tricornutum*. *Canadian Journal of Botany*, 83, 909–916. <https://doi.org/10.1139/B05-078>

Harada, H., Nakatsuma, D., Ishida, M., & Matsuda, Y. (2005). Regulation of the expression of intracellular β -carbonic anhydrase in response to CO₂ and light in the marine diatom *Phaeodactylum tricornutum*. *Plant Physiology*, 139, 1041–1050. <https://doi.org/10.1104/pp.105.065185>

Huang, W. M., Shao, H., Zhou, S. N., Zhou, Q., Fu, W. L., Zhang T., Jiang, H. S., Li, W., Gontero, B., & Maberly, S. C. (2018). Different CO₂ acclimation strategies in juvenile and mature leaves of *Ottelia alismoides*. *Photosynthesis Research*, 138, 219–232. <https://doi.org/10.1007/s11120-018-0568-y>

Iversen, L. L., Winkel, A., Bastrup-Spohr, L., Hinke, A. B., Alahuhta, J., Bastrup-Pedersen, A., Birk, S., Brodersen, P., Chambers, P. A., Ecke, F., Feldmann, T., Gebler, D., Heino, J., Jespersen, T. S., Moe, S. J., Riis, T., Sass, L., Vestergaard, O., Maberly, S. C., Sand-Jensen, K., & Pedersen, O. (2019). Catchment properties and the photosynthetic trait composition of freshwater plant communities. *Science*, 366, 878–881. <https://doi.org/10.1126/science.aay5945>

James, P. L., & Larkum, A. W. D. (1996). Photosynthetic inorganic carbon acquisition of *Posidonia australis*. *Aquatic Botany*, 55, 149–157. [https://doi.org/10.1016/S0304-3770\(96\)01074-1](https://doi.org/10.1016/S0304-3770(96)01074-1)

Jensen, E.L., Clement, R., Kosta, A., Maberly, S. C., & Gontero, B. (2019). A new widespread subclass of carbonic anhydrase in marine phytoplankton. *The ISME Journal*, 13, 2094–2106. <https://doi.org/10.1038/s41396-019-0426-8>

Karlsson, J., Clarke, A. K., Chen, Z. Y., Huggins, S. Y., Park, Y. I., Husic, H. D., Moroney, J. V., & Samuelsson, G. (1998). A novel alpha-type carbonic anhydrase associated with the thylakoid membrane in *Chlamydomonas reinhardtii* is required for growth at ambient CO₂. *EMBO Journal*, 17, 1208–1216. <https://doi.org/10.1093/emboj/17.5.1208>

Klavsén, S. K., Madsen, T. V., & Maberly, S. C. (2011). Crassulacean acid metabolism in the context of other carbon-concentrating mechanisms in freshwater plants: a review. *Photosynthesis Research*, 109, 269–279. <https://doi.org/10.1007/s11120-011-9630-8>

Klenell, M., Snoeijs, P., & Pedersén, M. (2004). Active carbon uptake in *Laminaria digitata* and *L. saccharina* (Phaeophyta) is driven by a proton pump in the plasma membrane. *Hydrobiologia*, 514, 41–53. <https://doi.org/10.1023/B:hydr.0000018205.80186.3e>

Larsson, C., & Axelsson, L. (1999). Bicarbonate uptake and utilization in marine macroalgae. *European Journal of Phycology*, 34, 79–86. <https://doi.org/10.1080/09670269910001736112>

- Maberly, S. C., & Spence, D. H. N. (1983). Photosynthetic inorganic carbon use by freshwater plants. *Journal of Ecology* , 71, 705–724. [https://doi.org/ 10.2307/2259587](https://doi.org/10.2307/2259587)
- Maberly, S. C. (1990). Exogenous sources of inorganic carbon for photosynthesis by marine macroalgae. *Journal of Phycology* , 26, 439–449. [https://doi.org/ 10.1111/j.0022-3646.1990.00439.x](https://doi.org/10.1111/j.0022-3646.1990.00439.x)
- Maberly, S. C. (1996). Diel, episodic and seasonal changes in pH and concentrations of inorganic carbon in a productive lake. *Freshwater Biology* , 35, 579–598. [https://doi.org/ 10.1111/j.1365-2427.1996.tb01770.x](https://doi.org/10.1111/j.1365-2427.1996.tb01770.x)
- Maberly, S. C., & Madsen, T. V. (1998). Affinity for CO₂ in relation to the ability of freshwater macrophytes to use HCO₃⁻. *Functional Ecology* , 12, 99–106. <http://www.jstor.org/stable/2390529>
- Maberly, S. C., & Gontero, B. (2017). Ecological imperatives for aquatic CO₂-concentrating mechanisms. *Journal of Experimental Botany* , 68, 3797–3814. [https://doi.org/ 10.1093/jxb/erx201](https://doi.org/10.1093/jxb/erx201)
- Maberly, S. C., & Gontero, B. (2018). Trade-offs and synergies in the structural and functional characteristics of leaves photosynthesizing in aquatic environments. In: Adams III, W. W., Terashima, I., eds. The leaf: a platform for performing photosynthesis. Advances in photosynthesis and respiration (Including bioenergy and related processes). Springer, Cham. 307–343. [https://doi.org/ 10.1007/978-3-319-93594-2_11](https://doi.org/10.1007/978-3-319-93594-2_11)
- Millhouse, J., & Strother, S. (1986). Salt-stimulated bicarbonate-dependent photosynthesis in the marine angiosperm *Zostera muelleri* . *Journal of Experimental Botany* , 37, 965–976. [https://doi.org/ 10.1093/jxb/37.7.965](https://doi.org/10.1093/jxb/37.7.965)
- Moroney, J. V., Husic, H. D., & Tolbert, N. E. (1985). Effect of carbonic anhydrase inhibitors on inorganic carbon accumulation by *Chlamydomonas reinhardtii* . *Plant Physiology* , 79, 177–183. [https://doi.org/ 10.1104/pp.79.1.177](https://doi.org/10.1104/pp.79.1.177)
- Moroney, J. V., & Chen, Z. Y. (1998). The role of the chloroplast in inorganic carbon uptake by eukaryotic algae. *Canadian Journal of Botany* , 76, 1025–1034. [https://doi.org/ 10.1139/b98-077](https://doi.org/10.1139/b98-077)
- Moroney, J. V., Bartlett, S. G., & Samuelsson, G. (2001). Carbonic anhydrases in plants and algae. *Plant Cell & Environment* , 24, 141–153. [https://doi.org/ 10.1111/j.1365-3040.2001.00669.x](https://doi.org/10.1111/j.1365-3040.2001.00669.x)
- Moroney, J. V., Ma, Y., Frey, W. D., Fusilier, K. A., Pham, T. T., Simms, T. A., DiMario, R. J., Yang, J., & Mukherjee, B. (2011). The carbonic anhydrase isoforms of *Chlamydomonas reinhardtii* : intracellular location, expression, and physiological roles. *Photosynthesis Research* , 109, 133–149. [https://doi.org/ 10.1007/s11120-011-9635-3](https://doi.org/10.1007/s11120-011-9635-3)
- Nakajima, K., Tanaka, A., & Matsuda, Y. (2013). SLC4 family transporters in a marine diatom directly pump bicarbonate from seawater. *Proceedings of the National Academy of Sciences USA* , 110, 1767–1772. [https://doi.org/ 10.1073/pnas.1216234110](https://doi.org/10.1073/pnas.1216234110)
- Poliner, E., Panchy, N., Newton, L., Wu, G., Lapinsky, A., Bullard, B., Zienkiewicz, A., Benning, C., Shiu, S. H., & Farré, E. M. (2015). Transcriptional coordination of physiological responses in *Nannochloropsis oceanica* CCM1779 under light/dark cycles. *Plant Journal* , 83, 1097–1113. [https://doi.org/ 10.1111/tpj.12944](https://doi.org/10.1111/tpj.12944)
- Prins, H. B. A., Snel, J. F. H., Helder, R. J., & Zanstra, P. E. (1980). Photosynthetic HCO₃⁻ utilization and OH⁻ excretion in aquatic angiosperms: light induced pH changes at the leaf surface. *Plant Physiology* , 66, 818–822. [https://doi.org/ 10.1104/pp.66.5.818](https://doi.org/10.1104/pp.66.5.818)
- Raven, J. A. (1970). Exogenous inorganic carbon sources in plant photosynthesis. *Biological Reviews* , 45, 167–221. <https://doi.org/10.1111/j.1469-185X.1970.tb01629.x>
- Roberts, R. J., Carneiro, M. O., & Schatz, M. C. (2013). The advantages of SMRT sequencing. *Genome Biology* , 14, 405. [https://doi.org/ 10.1186/gb-2013-14-6-405](https://doi.org/10.1186/gb-2013-14-6-405)
- Romero, M. F., Chen, A. P., Parker, M. D., & Boron, W. F. (2013). The SLC4 family of bicarbonate (HCO₃⁻) transporters. *Molecular Aspects of Medicine* , 34, 159–182. [https://doi.org/ 10.1016/j.mam.2012.10.008](https://doi.org/10.1016/j.mam.2012.10.008)

- Samukawa, M., Shen, C., Hopkinson, B. M., & Matsuda, Y. (2014). Localization of putative carbonic anhydrases in the marine diatom, *Thalassiosira pseudonana*. *Photosynthesis Research*, 121, 235–249. <https://doi.org/10.1007/s11120-014-9967-x>
- Satoh, D., Hiraoka, Y., Colman, B., & Matsuda, Y. (2001). Physiological and molecular biological characterization of intracellular carbonic anhydrase from the marine diatom *Phaeodactylum tricorutum*. *Plant Physiology*, 126, 1459–1470. <https://doi.org/10.1104/pp.126.4.1459>
- Shao, H., Gontero, B., Maberly, S. C., Jiang, H. S., Cao, Y., Li, W., & Huang, W. M. (2017). Responses of *Ottelia alismoides*, an aquatic plant with three CCMs, to variable CO₂ and light. *Journal of Experimental Botany*, 68, 3985–3995. <https://doi.org/10.1093/jxb/erx064>
- Sharkia, R., Beer, S., & Cabantchik, Z. I. (1994). A membrane-located polypeptide of *Ulva* sp. which may be involved in HCO₃⁻ uptake is recognized by antibodies raised against the human red-blood-cell anion-exchange protein. *Planta*, 194, 247–249. <https://doi.org/10.1007/BF00196394>
- Silva, T. S. F., Melack, J. M., & Novo, E. M. L. M. (2013). Responses of aquatic macrophyte cover and productivity to flooding variability on the Amazon floodplain. *Global Change Biology*, 19, 3379–3389. <https://doi.org/10.1111/gcb.12308>
- Sowah, D., & Casey, J. R. (2011). An intramolecular transport metabolon: fusion of carbonic anhydrase II to the COOH terminus of the Cl⁻/HCO₃⁻ exchanger, AE1. *American Journal of Physiology-Cell Physiology*, 301, C336–C346. <https://doi.org/10.1152/ajpcell.00005>. 2011
- Staal, M., Elzenga, J. T. M., & Prins, H. B. A. (1989). ¹⁴C fixation by leaves and leaf cell protoplasts of the submerged aquatic angiosperm *Potamogeton lucens*: carbon dioxide or bicarbonate? *Plant Physiology*, 90, 1035–1040. <https://doi.org/10.1104/pp.90.3.1035>
- Steemann-Nielsen, E. (1947). Photosynthesis of aquatic plants with special reference to the carbon sources. *Dansk Botanisk Arkiv Udgivet af Dansk Botanisk Forening*, 8, 3–71.
- Sterling, D., Reithmeier, R. A. F., & Casey, J. R. (2001). A transport metabolon: Functional interaction of carbonic anhydrase II and chloride/bicarbonate exchangers. *The Journal of Biological Chemistry*, 276, 47886–47894. <https://doi.org/10.1074/jbc.M105959200>
- Tachibana, M., Allen, A. E., Kikutani, S., Endo, Y., Bowler, C., & Matsuda, Y. (2011). Localization of putative carbonic anhydrases in two marine diatoms, *Phaeodactylum tricorutum* and *Thalassiosira pseudonana*. *Photosynthesis Research*, 109, 205–221. <https://doi.org/10.1007/s11120-011-9634-4>
- Thornell, I. M., & Bevenssee, M. O. (2015). Regulators of *Slc4* bicarbonate transporter activity. *Frontiers in Physiology*, 6, 166. <https://doi.org/10.3389/fphys.2015.00166>
- Tsuji, Y., Nakajima, K., & Matsuda, Y. (2017). Molecular aspects of the biophysical CO₂-concentrating mechanism and its regulation in marine diatoms. *Journal of Experimental Botany*, 68, 3763–3772. <https://doi.org/10.1093/jxb/erx173>
- van Hille, R., Fagan, M., Bromfield, L., & Pott, R. (2014). A modified pH drift assay for inorganic carbon accumulation and external carbonic anhydrase activity in microalgae. *Journal of Applied Phycology*, 26, 377–385. <https://doi.org/10.1007/s10811-013-0076-6>
- Zhang, Y. Z., Yin, L. Y., Jiang, H. S., Li, W., Gontero, B., & Maberly, S. C. (2014). Biochemical and biophysical CO₂ concentrating mechanisms in two species of freshwater macrophyte within the genus *Ottelia* (Hydrocharitaceae). *Photosynthesis Research*, 121, 285–297. <https://doi.org/10.1007/s11120-013-9950-y>
- Zou, D. H., & Gao, K. S. (2010). Acquisition of inorganic carbon by *Endarachne binghamiae* (Scytosiphonales, Phaeophyceae). *European Journal of Phycology*, 45, 117–126. <https://doi.org/10.1080/09670260903383909>

Figure legends

Figure 1. Example of a typical pH-drift over time (one replicate) for *O. alismoides* tested at an initial alkalinity of 1 mequiv L⁻¹ without (control) or with inhibitors (AZ, DIDS).

Figure 2. Analysis of pH drift experiments without (control) or with inhibitors (AZ and DIDS) in *O. alismoides*. (a) Final pH; (b) Final CO₂ concentration; (c) Initial slope of Ci uptake rate vs concentration of CO₂ (between 15~40 μM), α_C; (d) CO₂ compensation point (CP(CO₂)); (e) C_T/Alk. Values represent means ± SE, n=3. Letters indicate statistical differences between control and treatments (one-way ANOVA, Duncan's and Tukey's post-hoc tests P<0.05).

Figure 3. Effect of AZ or DIDS on the Ci uptake rate at different CO₂ concentrations in *O. alismoides*. (a) Ci uptake rate; (b) Ci uptake inhibition. Values represent means ± SE, n=3. Letters in (a) indicate statistical differences among control and inhibitor treatments within CO₂ concentrations (one-way ANOVA, Duncan's and Tukey's post-hoc tests P<0.05). Letters and symbols in (b) indicate statistical differences among different CO₂ concentrations within inhibitor treatment (Mann-Whitney test P<0.05).

Figure 4. Effect of removal of AZ on Ci uptake rate in *O. alismoides* leaves at different CO₂ concentrations. Values represent means ± SE, n=3. (a) 0.1 mM AZ; (b) 0.2 mM AZ. The inhibitor was removed by washing the treated leaves in the post-control (see Methods). Letters indicate statistical differences between the control and inhibitor treatments of AZ for each CO₂ concentration (one-way ANOVA, Duncan's and Tukey's post-hoc tests P<0.05).

Figure 5. Effect of AZ and DIDS on Ci uptake rate and external CA activity in leaves of *O. alismoides* acclimated to high CO₂ (HC) or low CO₂ (LC) and measured at an initial CO₂ concentration of 12 μM. (a) Ci uptake rate; (b) Inhibition of Ci uptake rate; (c) External CA activity and (d) Inhibition of external CA activity. Values represent means ± SE, n=3. For panels (a) and (c), letters indicate statistical differences between the control and different treatments at HC and LC acclimated leaves using one-way ANOVA, Duncan's and Tukey's post-hoc tests P<0.05. For panels (b) and (d), uppercase and lowercase letters indicate statistical differences among inhibitor treatments at HC and LC respectively using the Mann-Whitney test P<0.05; the line above the two columns indicates the statistical differences between HC and LC treatments (Mann-Whitney test P<0.05).

Figure 6. Phylogenetic tree of αCA-1 isoforms, prediction of location for αCA-1 peptides, and mRNA expression for αCA-1 and SLC4 HCO₃⁻ transporters in *O. alismoides* leaves acclimated at high CO₂ (HC) and low CO₂ (LC) concentrations. (a) Phylogenetic tree of αCA-1 isoforms in *O. alismoides*; (b) Output of the predicted location tested on the four isoforms for putative αCA-1 from the Target P server; (c) mRNA expression for αCA-1; (d) mRNA expression for SLC4 HCO₃⁻ transporters. In panel (a), the scale bar at the bottom represents the evolutionary distances in amino acid sequences. In panel (b), cTP is the chloroplast transit peptide, mTP is the mitochondrial targeting peptide, SP is the secretory pathway, Other stands for other locations, Loc gives the final prediction, RC is the reliability class (from 1 to 5), where 1 indicates the strongest prediction. The default was used to choose cutoffs for the predictions. Values in panels (c) and (d) represent the mean ± SE, n=3. Data of SLC4 HCO₃⁻ transporters expression in panel (d) correspond to the highest expressed transcript. The lines in panels (c) and (d) above the two columns indicate the statistical differences between LC and HC treatment (one-way ANOVA, P<0.05).

Figure 7. A model of inorganic carbon acquisition in *O. alismoides*. (a) Model structure. passive diffusion of CO₂; diffusion of HCO₃⁻ and conversion to CO₂ by αCA-1 at the plasmalemma; diffusion of HCO₃⁻ and transfer across the plasmalemma by SLC4 HCO₃⁻ transporters. (b) The contribution of CO₂-diffusion, diffusion of HCO₃⁻ and conversion to CO₂ via αCA-1 and transfer of HCO₃⁻ by SLC4 HCO₃⁻ transporters to total Ci uptake at different CO₂ concentrations.

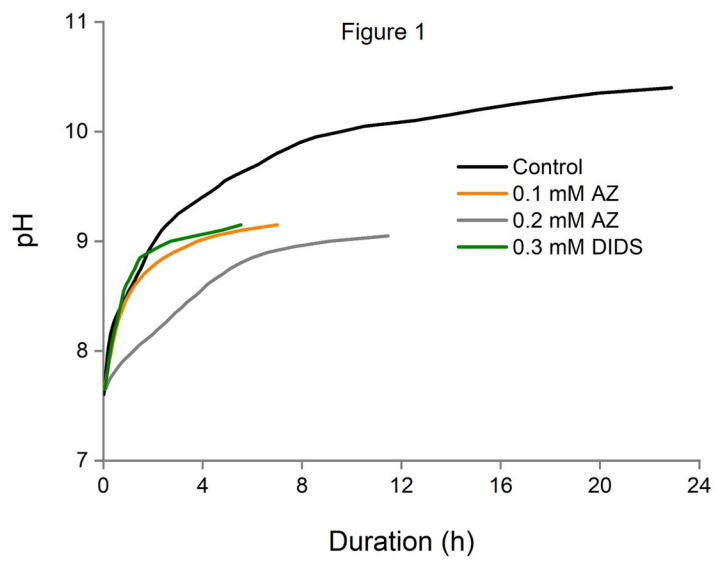
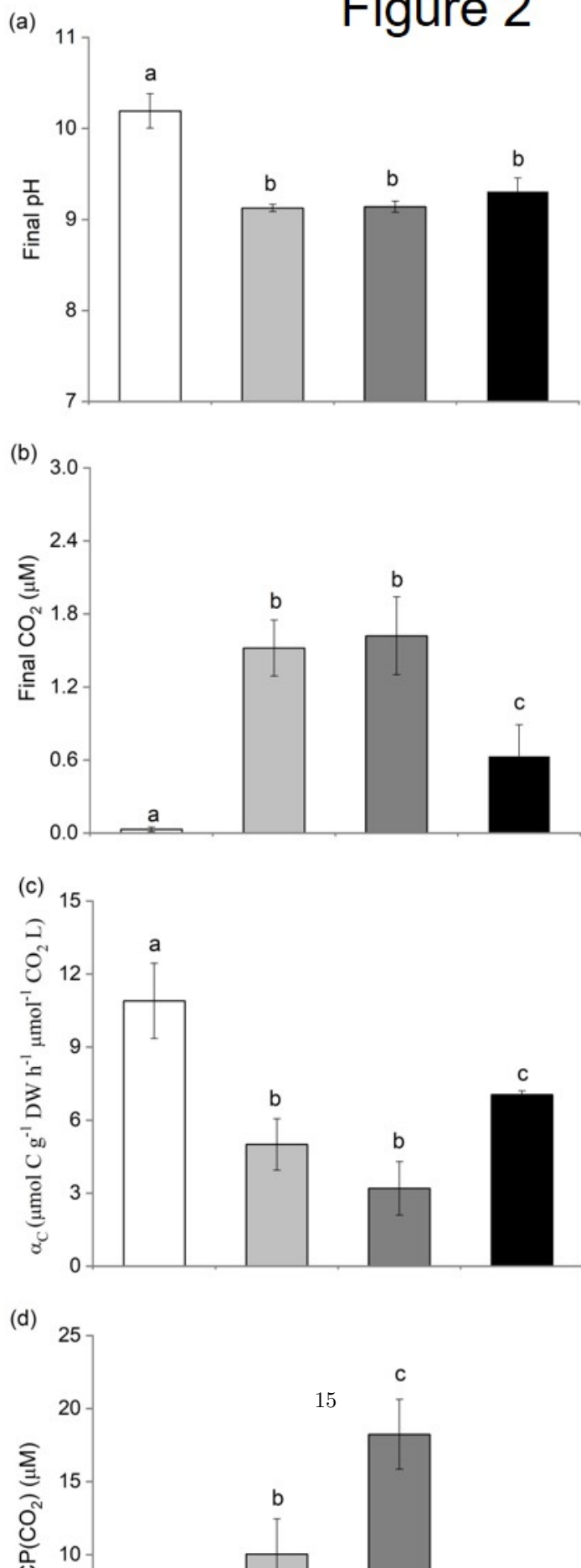


Figure 2



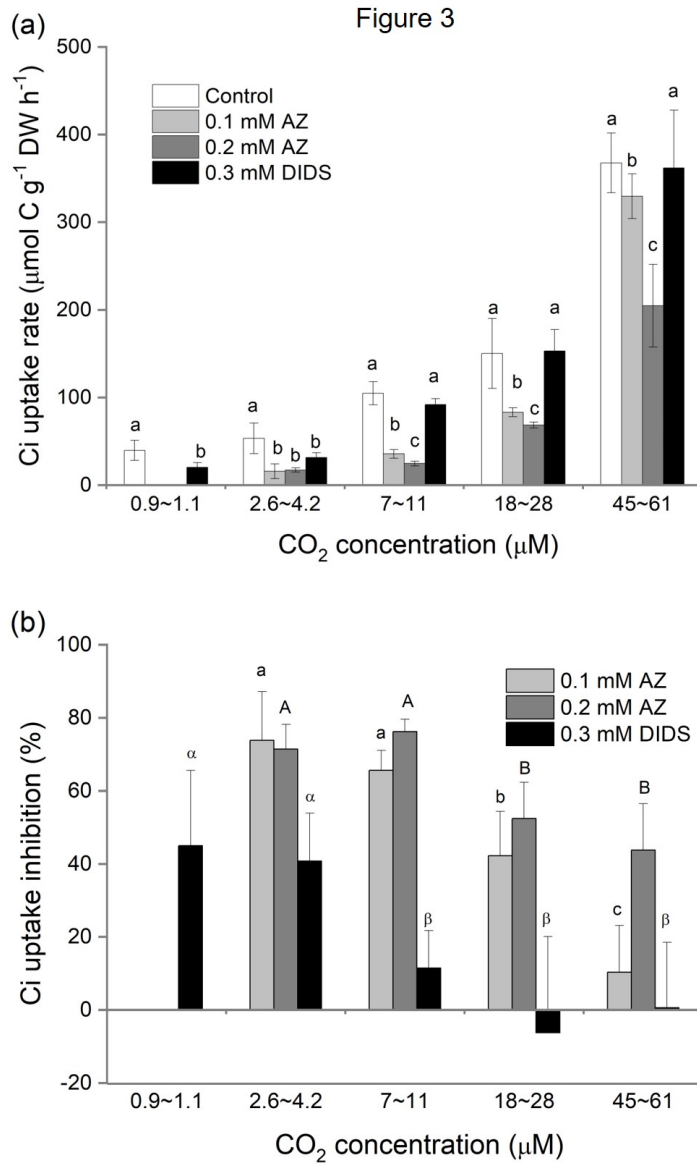


Figure 4

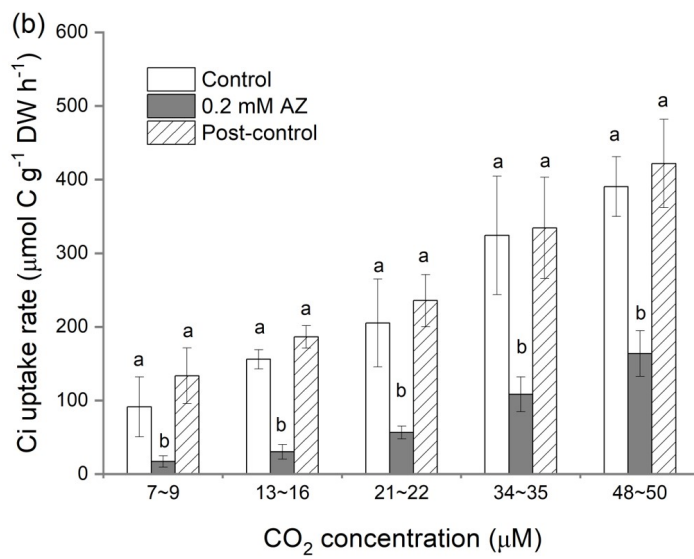
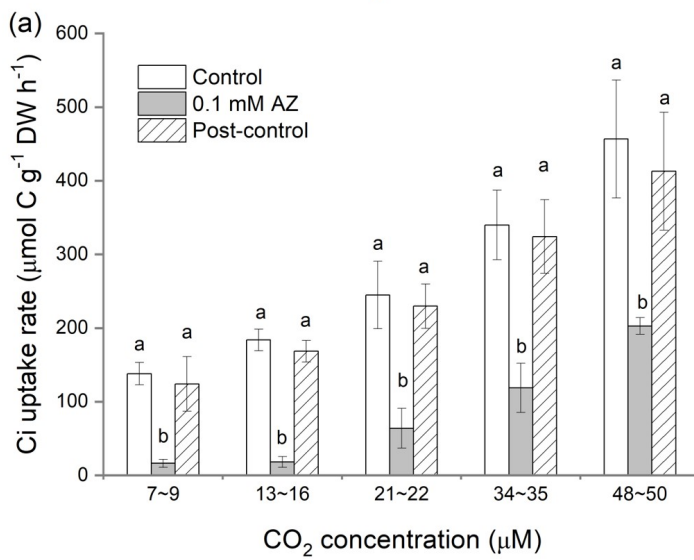


Figure 5

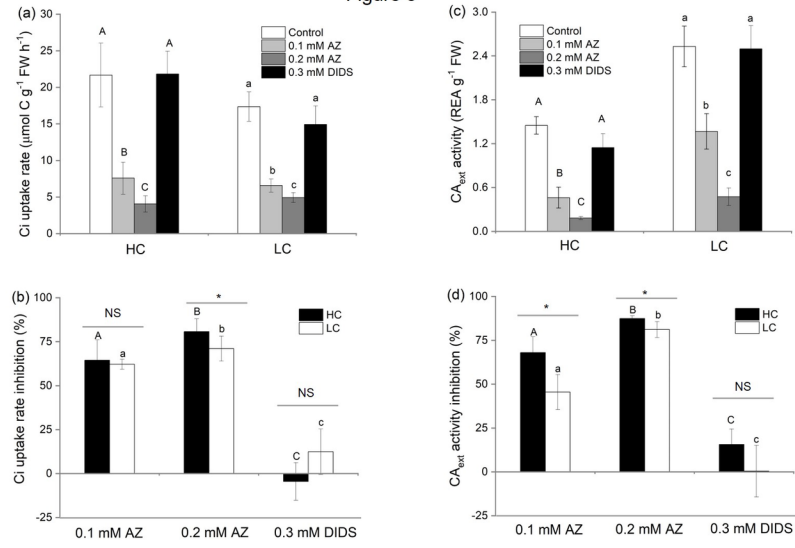
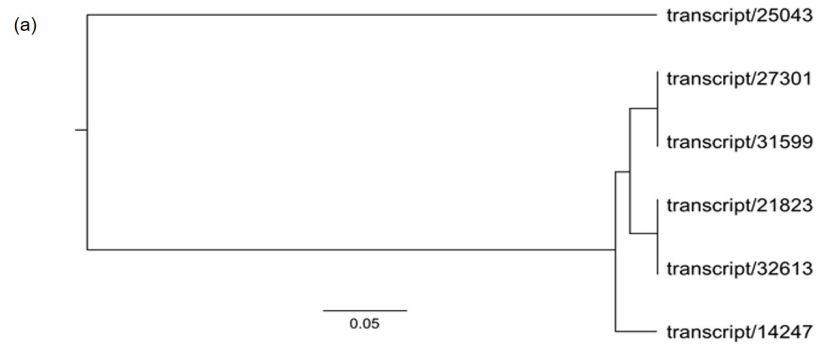


Figure 6



(b)

Putative protein	Isoforms	cTP	mTP	SP	Other	Loc	RC
α CA-1	1	0.077	0.025	0.885	0.013	SP	1
α CA-1	2	0.023	0.023	0.951	0.050	SP	1
α CA-1	3	0.021	0.025	0.952	0.054	SP	1
α CA-1	4	0.023	0.023	0.951	0.050	SP	1

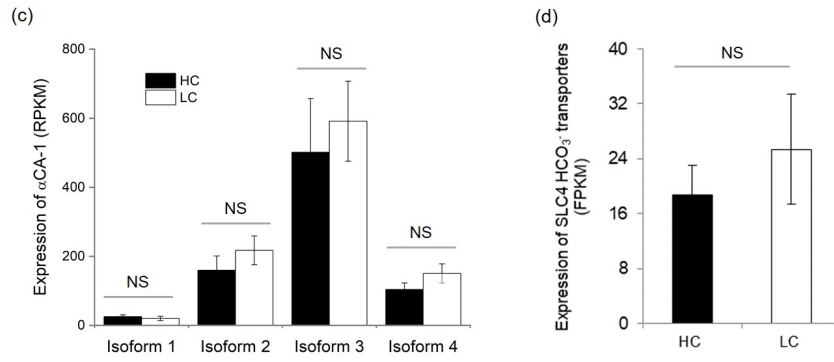


Figure 7

